

Analytical Methods

Accepted Manuscript



This is an *Accepted Manuscript*, which has been through the Royal Society of Chemistry peer review process and has been accepted for publication.

Accepted Manuscripts are published online shortly after acceptance, before technical editing, formatting and proof reading. Using this free service, authors can make their results available to the community, in citable form, before we publish the edited article. We will replace this *Accepted Manuscript* with the edited and formatted *Advance Article* as soon as it is available.

You can find more information about *Accepted Manuscripts* in the [Information for Authors](#).

Please note that technical editing may introduce minor changes to the text and/or graphics, which may alter content. The journal's standard [Terms & Conditions](#) and the [Ethical guidelines](#) still apply. In no event shall the Royal Society of Chemistry be held responsible for any errors or omissions in this *Accepted Manuscript* or any consequences arising from the use of any information it contains.

1
2
3
4
5
6
7
8
9
10
11
12
13
14
15
16
17
18
19
20
21
22
23
24
25
26
27
28
29
30
31
32
33
34
35
36
37
38
39
40
41
42
43
44
45
46
47
48
49
50
51
52
53
54
55
56
57
58
59
60

1 **Rapid and nondestructive evaluation of fish Freshness by near infrared**
2 **reflectance spectroscopy combined with chemometrics analysis**

3 ¹Ran Ding, ¹Xingyi Huang*, ¹Fangkai Han, ¹Huang Dai, ^{1,2}Ernest Teye, ¹Fubin Xu

4 ¹School of Food and Biological Engineering, Jiangsu University,

5 Xuefu Road 301, Zhenjiang 212013, Jiangsu, P. R. China

6 ²School of Agriculture, Department of Agricultural Engineering,

7 University of Cape Coast, Cape Coast, Ghana

8 *Corresponding author: Xingyi Huang, Email: h_xingyi@163.com

9 Tel: +86-51188792368, Fax: +86-51188797308

10 **Abstract**

11 Rapid and nondestructive measurement of freshness is essential for control of fish
12 and its products' quality and safety. In this study, K value was measured by high
13 performance liquid chromatography (HPLC) and employed as an index of fish
14 freshness. The prediction models of the silver chub freshness were developed using
15 Fourier Transform Near Infrared Reflectance Spectroscopy (FT-NIRS) with Several
16 Partial Least Squares (PLS, i-PLS, Si-PLS), Support Vector Machines Regression
17 (SVMR) and Synergy interval plus Support vector machine regression leading to
18 Si-SVMR. By comparison, the performance of Si-SVMR model was superior to the
19 others for the prediction of K value, where RMSECV = 0.027095 and Rc = 95.59%
20 for calibration set, while RMSEP = 0.036525 and Rp = 93.74% for prediction set. The
21 results indicated that FT-NIR spectroscopy together with Si-SVMR model could be a
22 reliable method for detection of fish freshness.

23 Keywords: NIRS, fish freshness, K value, SVMR

24 **1.0 Introduction**

25 It is well known that freshness is the primary characteristic of the quality of
26 freshwater fish and a positive property well evaluated by consumers. Loss of
27 freshness and spoilage of fish are complicated processes and various factors such as
28 fishing, handling, bleeding, storage temperature, the kind of fish species, the amount
29 of food in the guts influence the spoilage pattern. The traditional detection methods of
30 fish freshness mainly include sensory evaluation, microbiological, chemical, and

1
2
3
4 31 physical testing methods. Sensory evaluation methods based on significant
5
6 32 appearance parameters such as, skin, slime, eyes, gills, belly and odor are conducted
7
8 33 by experienced and well-trained humans(Nollet and Toldra 2010). Although these
9
10 34 methods can be done without damage to the fish, these are subjective due to the
11
12 35 subjective opinion of human judges and difficult to make quantitative
13
14 36 analysis(Pons-Sánchez-Cascado, Vidal-Carou et al. 2006). At present microbiological
15
16 37 methods based on total viable counts, chemical and biochemical methods (total
17
18 38 volatile basic nitrogen, trimethylamine, pH, ATP, etc.), and physical testing methods
19
20 39 play a key role in industrial fish quality and safety evaluation and inspection. Even
21
22 40 certain of them have been used as regulation methods and gold standards serving
23
24 41 scientific researches with their reliability and accuracy (Watanabe, Tamada et al. 2005,
25
26 42 Alimelli, Pennazza et al. 2007, Zaragoza, Ribes et al. 2012). However, these methods
27
28 43 are normally expensive, time-consuming, laborious, destructive and difficult for the
29
30 44 application of the real-time detection. Recently emerging sensor array technologies,
31
32 45 such as electronic tongue, electronic nose and olfaction visualization technology, were
33
34 46 also used for the study of freshness detection. These methods have their advantages.
35
36 47 Nevertheless, gas gathering, complicated testing procedures and moisture sensibility
37
38 48 weaken the overall performance for electronic nose technology. Electronic tongue
39
40 49 technology is not suitable for online testing due to the troublesome liquid sample
41
42 50 preparation. As for olfaction visualization technology, the colorimetric sensor array
43
44 51 preparation is a time-consuming effort and expensive metalloporphyrins directly
45
46 52 result in the increase of detection cost (Gil, Barat et al. 2008, Huang, Xin et al. 2011,
47
48 53 Ruiz-Rico, Fuentes et al. 2013). Therefore, it is necessary to develop a simple, fast,
49
50 54 non-destructive, objective, economical and quantitative method for the detection of
51
52 55 fish freshness (Wei and Wu 2007, Dowlati, de la Guardia et al. 2012).

56
57
58
59
60
Near infrared reflectance spectroscopy (NIRS) is the high-tech analytical techniques in the field of analytical chemistry. It is the integration of multi-disciplinary knowledge, such as spectroscopy, chemometrics, and computer multi-disciplinary knowledge and others. This method is simple, fast, green, low cost and has a good reproducibility. The root of modern near infrared analytical techniques

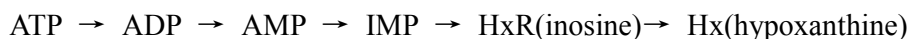
1
2
3
4 61 began earlier in the 1960s by the American Scientist Norris for Agriculture product
5
6 62 quality measurement. This technology was usually used for a measurement of
7
8 63 agricultural moisture, fat, protein and other substances(Khodabux, L'Omelette et al.
9
10 64 2007, Tito, Rodemann et al. 2012). With the rapid development of computer
11
12 65 technology and the stoichiometry, the technology has been applied to various walks of
13
14 66 life, such as pharmaceutical analysis(Porfire, Rus et al. 2012) , chemical
15
16 67 engineering(Ribeiro, Raja et al. 2014), environmental science (Buerck, Roth et al.
17
18 68 2001), agricultural products quality researches (Nicolai, Beullens et al. 2007).

19
20 69 The previous research objects of the detection of fish freshness with NIRS mostly
21
22 70 were with fish fillets and surimi (Bøknæs, Jensen et al. 2002, Xu, Huang et al. 2012),
23
24 71 with the fish body broken. Recently the back of the entire fish was also studied
25
26 72 (Zhang, Xu et al. 2011, Li, Wang et al. 2013). Remarkably, the back of fish is covered
27
28 73 by fish scales which are mainly composed of CaO, P₂O₅ and Collagen(Atta 2013).
29
30 74 Normally, Inorganic Chemical (CaO, P₂O₅) has reflection interference on NIRS.
31
32 75 Besides, NIRS may be also interfered with the different distribution of organs and
33
34 76 fishbone in the abdominal cavity of fish. NIRS detection technology of large yellow
35
36 77 croaker by removing fish scales based on PLS methods was proposed (Zhang, Xu et
37
38 78 al. 2011). The result is ideal, but the method is also destructive. In contrast, the
39
40 79 structure of fish eye is sample and easy to locate(Dowlati, Mohtasebi et al. 2013),
41
42 80 which bring about a good test repeatability. Fish eye gradually becomes cloudy from
43
44 81 the clear, until the corruption and collapse the storage duration, which is a sound
45
46 82 determination indicator of fish freshness for consumers and fish merchants. Hence,
47
48 83 NIR detection method based on fish eye could be rapid, simple, nondestructive and
49
50 84 easy to locate in theory.

51
52 85 Recently, a new perspective that K value is a more accurate index for the early
53
54 86 freshness of fish than TVBN (Total Volatile Basic Nitrogen) was put forward. In the
55
56 87 view, the freshness of fish depends primarily on its own biochemical reactions. That a
57
58 88 series of biochemical reactions occurred after death is the essence of the change of
59
60 89 fish freshness and has nothing to do with the microbial decomposition. The microbial
90
91 90 decomposition occurred in the late stage of fish deterioration. The decomposition of

1
2
3
4
5
6
7
8
9
10
11
12
13
14
15
16
17
18
19
20
21
22
23
24
25
26
27
28
29
30
31
32
33
34
35
36
37
38
39
40
41
42
43
44
45
46
47
48
49
50
51
52
53
54
55
56
57
58
59
60

91 ATP in fish meat sets in after death, and its compounds are subsequently produced
92 according to the following sequence.



94 The K value represents the proportion (%) of the total amount of inosine and
95 hypoxanthine relative to that of ATP-related compounds. The higher the K value, the
96 less fresh the fish. ATP had a rapid degradation from the dead to rigor mortis, leading
97 to a sharp increase of K value. Hence, K value is a more accurate index for the early
98 freshness of fish than TVBN([Etsuo Watanabe 2005](#)). The researches on horse
99 mackerel([Losada, Piñeiro et al. 2005](#)), trout ([Bizri, Bouhours et al. 1985](#)), yellow fin
100 tuna([Kamalakanth, Ginson et al. 2011](#)) and other during iced storage([Lougovois,](#)
101 [Kyranas et al. 2003](#)) showed that K value could be used as an important chemical
102 indicator for the evaluation of fish freshness.

103 Freshwater fish is popular with consumers because of its delicacy and nutrition.
104 Silver carp (*Hypophthalmichthys molitrix*) is a widespread species of freshwater fish
105 in China. In this study, NIRS was attempted for the detection of K value in silver carp
106 during storage and preservation. In addition, HPLC was employed for K value
107 measurement of silver carps. Multiple spectral preprocessing methods were compared.
108 PCA algorithm was applied for dimensionality reduction. Several partial least square
109 techniques were applied (PLS, i-PLS, Si-PLS). Support Vector Machine Regression
110 and Synergy interval plus Support vector machine regression leading to Si-SVMR
111 were also acquired for the quantitative prediction of K value of silver carp.

112 **2.0 Materials and methods**

113 **2.1 Silver carp samples**

114 180 fresh silver carps (*Hypophthalmichthys molitrix*) were purchased from
115 Zhenjiang fish market with an average weight of 950 g and average body length of 40
116 cm. The fish were washed with running water and then put into food preservation kits
117 with labels (1~180). **Then all fish were stored in a refrigerator at about 4°C. 15 fish**
118 **were selected randomly for the spectral collection every day and then they were**
119 **slaughtered for the measurement of K values. The test was conducted for 12 days.**

120 **2.2. NIR instrumentation and data collection**

1
2
3
4 121 The spectrum of each sample was collected in the reflectance mode using the
5
6 122 Antaris II Near Infrared Spectrophotometer (Thermo Electron Company, USA) with
7
8 123 an integrating sphere. Built-in background was as a reference. Each eye of the fish
9
10 124 was scanned 5 times. The average of 10 data was used as the final raw data of the fish.
11
12 125 The spectra of 15 fish were collected one by one every day. Each time a fish was
13
14 126 taken out of the fridge for the spectral collection. After the spectral collection of the
15
16 127 fish was finished, it was transferred to the next laboratory in an ice box for the
17
18 128 measurement of K value. The whole experiment was conducted at an ambient
19
20 129 temperature of $25 \pm 1^\circ\text{C}$ and the air humidity was kept at steady state. Each spectrum
21
22 130 was an average of 16 scans with a spectral range of $10,000\text{--}4000\text{ cm}^{-1}$, and the raw
23
24 131 data set were measured in the interval of 8 cm^{-1} , resulting in 1557 variables. The raw
25
26 132 NIRS profile of a silver carp is shown in Fig.1.

26 133 **2.3. Determination of K value**

27
28 134 K value is an indicator of the fish freshness. The researches on horse
29
30 135 mackerel(Losada, Piñeiro et al. 2005), trout(Bizri, Bouhours et al. 1985), yellow fin
31
32 136 tuna(Kamalakanth, Ginson et al. 2011) and other during iced storage(Lougovois,
33
34 137 Kyranas et al. 2003) showed that K value could be used as an important chemical
35
36 138 indicator for the evaluation of fish freshness. It equals to the percentage of the sum of
37
38 139 inosine and hypoxanthine and the total of adenosine triphosphoric (ATP) and its
39
40 140 decomposition product. Expressed as(Losada, Piñeiro et al. 2005, Kimiya, Sivertsen
41
42 141 et al. 2013):

$$43 \quad K(\%) = \frac{100 \times (HxR + Hx)}{ATP + ADP + AMP + IMP + HxR + Hx} \quad (1)$$

44
45 143 ATP—adenosine triphosphate ,

46
47 144 ADP—adenosine diphosphate ,

48
49 145 AMP—adenosine monophosphate,

50
51 146 IMP—inosine monophosphate,

52
53 147 HxR—inosine,

54
55 148 Hx—hypoxanthine .

56
57 149 All concentration unit were $\mu\text{mol} / \text{g}$.

1
2
3 150 The fish was immediately slaughtered for the measurement of K values after its
4 151 near-infrared spectral collected. Specific steps are described below:

5 152 The flesh of fish back without scales was ground into minced fish with the mincing
6 machine. 1g of minced fish was homogenized with 10mL of purified water for 1 min.
7 153 20mL of 15% PCA(perchloric acid solution) was added to the mixture , keeping on
8 154 stirring for 5 min. Then the sample was centrifuged and supernatant was poured into a
9 155 beaker (100mL). The sediment was washed by 5% PCA and further was centrifuged.
10 156 Afterwards, the first and the second supernatant were merged. Repeat the above twice.
11 157

12 158 The supernatant was neutralized (pH 6.8) by adding 5M KOH , standing in an ice
13 159 bath for 30 min. Then the solution was centrifuged and the supernatant was poured
14 160 into 100-mL volumetric flask. The sediment was washed by 5% PCA-KOH. The
15 161 first and the second supernatant were merged and transferred into the above
16 162 volumetric flask. Repeat the above twice.

17 163 Finally, the solution in the 100-mL volumetric flask was diluted with purified water
18 164 to 100 mL and agitated, standing in the an ice bath in a short time.

19 165 Centrifugation conditions: 9000r/min, 10°C, 10min.

20 166 Liquid chromatography conditions:

21 167 1) high performance liquid chromatography (Ultimate 3000 DIONEX company in
22 168 Germany), C18 reverse phase column (Shimadzu inertsustain C18 4.6 × 150 mm,
23 169 5µm),

24 170 2) mobile phase: 0.05M disodium hydrogen phosphate-the phosphodiesterase sodium
25 171 hydroxide buffer (pH 6.8),

26 172 3) detection time : 30 min,

27 173 4) detection wavelength: 254 nm,

28 174 5) flow rate: 0.8mL/min,

29 175 6) column temperature: 2600°C.

30 176 The types and concentration of the single standard and mixed standard solution of
31 177 ATP , ADP, AMP, IMP, HxR and Hx were measured under the same conditions. The
32 178 standard curve was drawn. Fig.2. shows High Performance Liquid Chromatogram
33 179 (HPLC) of the standard ATP-related compounds. The types and concentration of the
34 180 standard samples were determined by comparing the retention time and peak area of
35 181 samples with standards. K value was calculated according to the method described
36 182 elsewhere(Kimiya, Sivertsen et al. 2013). The variation trend of K value of silver
37 183 chub during the cold storage was shown in Fig. 3.

38 184 **2.4 Chemometric methods and evaluation index**

39 185 All computations, chemometric analysis and graphics were executed with
40 186 programs developed in Matlab 2008b (The Mathworks, Inc., Natick, MA, USA). The
41 187 SVMR models were fitted using the functions provided in the libsvm-mat-2.89-3
42 188 toolbox.

43 189 The chemometric techniques was used in the research, including Savizky—Golay
44 190 polynomial curve smoothing (SG), 1st derivation(D1), Principal Component Analysis

1
2
3 191 (PCA), Support Vector Machine Regression (SVMR) and multifarious Partial Least
4
5 192 Squares (PLS, i-PLS, Si-PLS).

6
7 193 The application of SG-D1 is beneficial not only for the removal of noise but also
8
9 194 for extending the differences of characteristics(Xu, Xie et al. 2011, Chen, Ding et al.
10
11 195 2012). Compared with Partial Least Squares (PLS), Synergy Interval Partial Least
12
13 196 Squares (Si-PLS) needs the less number of spectra variables but the result is not less
14
15 197 than the result from PLS model in general(Chen, Zhao et al. 2007, Godoy, Vega et al.
16
17 198 2014, Teye, Huang et al. 2014). Support Vector Machine (SVM) determines the
18
19 199 appropriate trade-off between learning ability of limited samples and the learn
20
21 200 **accuracy** of specific samples for the best generalization performance (Devos,
22
23 201 Ruckebusch et al. 2009, Alves and Poppi 2013).

24
25 202 Root mean square error of cross-validation (RMSECV), Root mean squared error
26
27 203 of prediction (RMSEP) and Correlation coefficient (R) were employed as index for
28
29 204 the performance of the achieved model. The smaller RMSECV and RMSEP were, the
30
31 205 stronger the predictive ability of the achieved model was. The higher the similarity of
32
33 206 measurements and prediction values will make the R output move further towards 1,
34
35 207 leading to the stronger predictive ability of the achieved model(Chen, Zhao et al. 2009,
36
37 208 Teye, Huang et al. 2013).

37 209 **2.5 Calibration and prediction set**

38
39 210 On the first day, due to the difference of the silver carp vitality, the time of their
40
41 211 death was different after they were placed into the refrigerator. That brought large
42
43 212 differences on K value of the first day. Some fish stayed alive corresponding to K
44
45 213 value but others did not. Considering that the freshness of dead fish was studied in the
46
47 214 paper, the data from the next day to the twelfth day (**a total of 11 days**) were used for
48
49 215 modeling. The samples were divided into two sets, namely calibration set and
50
51 216 prediction set. The calibration set was made up of 110 samples and these samples
52
53 217 were used to model. 55 samples were used as the prediction set, which was used to
54
55 218 test the reliability and stability of the model. To minimize the error and avoid bias in
56
57 219 the division of the subsets, the data is rearranged according to the size of K value
58
59 220 from low to high order. Then in every 3 samples, two were selected as calibration set
60

1
2
3
4
5
6
7
8
9
10
11
12
13
14
15
16
17
18
19
20
21
22
23
24
25
26
27
28
29
30
31
32
33
34
35
36
37
38
39
40
41
42
43
44
45
46
47
48
49
50
51
52
53
54
55
56
57
58
59
60

221 and 1 as the prediction set.

222 **2.6 Quantification models**

223 Multifarious Partial Least Squares (PLS, i-PLS, Si-PLS), SVMR and Si-SVMR
224 models were applied for the prediction of K value of silver carps during the cold
225 storage. Firstly, multiple pretreatment methods and combination between them were
226 compared, including Savitzky-Golay (SG), First Derivative (D1), Second Derivative
227 (D2), Standard Normal Variate (SNV), Multiplicative Scatter Correction (MSC) and
228 Mean Centre (MC) as well as the combination of SG and D1. The selection principle
229 was based on maximal correlation coefficient (R). Then PLS with the full spectrum,
230 i-PLS and Si-PLS quantitative models were respectively achieved. And the efficient
231 joint intervals were also generated by Si-PLS model. Next, Principal Component
232 Analysis (PCA) was used for dimensionality reduction and then SVMR model with
233 the full spectra and the optimal combined subintervals from Si-PLS model were
234 respectively obtained.

235 **3.0 Results and discussion**

236 **3.1K value analysis**

237 ATP in the fish flesh would be degraded as: $ATP \rightarrow ADP \rightarrow AMP \rightarrow IMP \rightarrow$
238 $HxR \rightarrow Hx$ after the death of fish. K value is more accurate to indicate the changes in
239 the early stage (freshness) of fish than TVBN (Total Volatile Basic Nitrogen). Because
240 the rapid ATP decomposition leads to the soar of K value. However, the rate of protein
241 degradation is slow from the death of fish to final decay. The lower the K value, the
242 more fresh the fish. Inversely, the higher the K value, the less fresh the fish. There are
243 many studies on the relationship between K value and fish freshness (Lougovois,
244 Kyranas et al. 2003, Losada, Piñeiro et al. 2005, Kamalakanth, Ginson et al. 2011). It
245 is generally acknowledged that K value of live fish is not more than 10%; K value of
246 the secondary freshness range from 20% to 40%; the fish is inedible/harmful when the
247 K value is more than 40% (Khodabux, L'Omelette et al. 2007).

248 In this work, the behavior of K value during cold storage is shown in Fig.1. K
249 value is on the rise with the storage duration, with a sharp increase especially in the
250 first three days. The silver carps were fresh food with an average K value of 10.64%

1
2
3 251 on the first day. K values of some fish were less than 10%, indicating that the fish
4
5 252 were still dying on the first day. And K value of the death on the first day ranged from
6
7 253 10% to 20%, suggesting that they were fresh. On the second day silver carps were
8
9 254 also fresh with average K value of 19.67%. The silver carps were the secondary
10
11 255 freshness with an average K value of 20%~40% from the third to seventh days. The
12
13 256 fish is inedible starting from the eighth day. The perception of spoilage happened on
14
15 257 the twelfth day(Kimiya, Sivertsen et al. 2013).

16 258 **3.2 NIR examination**

17
18 259 Many factors have an effect on spectral response values in the process of
19
20 260 measurement, including high frequency random noise, baseline drift, signal to
21
22 261 background, uneven concentration, light scattering, or the optical path change and
23
24 262 others. Spectra preprocessing is very important in near infrared spectroscopy analysis
25
26 263 for the decrease of error. Multiple preprocessing methods were investigated
27
28 264 combining with Si-PLS model, including Savitzky-Golay polynomial curve smoothing
29
30 265 (SG), 1st derivation (D1), 2nd derivation (D2), Standard Normal Variate (SNV),
31
32 266 Multiplicative Scatter Correction (MSC) and Mean centering (MC) as well as SG-D1.
33
34 267 A SG filter with five smoothing points was employed to smooth and remove random
35
36 268 noise from NIR spectra. D1 and D2 of the spectra were also used to increase the
37
38 269 spectral resolution and to solve problems of baseline shift and linear tilt. MSC and
39
40 270 SNV were used to correct both multiplicative and additive effects of the spectra due to
41
42 271 scattering, light scattering, particle size, and the change of optical path. In MSC, each
43
44 272 spectrum was linearized to the average spectrum. Moreover, SNV was conducted by
45
46 273 normalizing each individual spectrum to zero mean and unit variance (Jamshidi,
47
48 274 Minaei et al. 2012). The arbitrary origin of interval scale variables can be eliminated
49
50 275 by MC. From Tab.1, the result of SG-D1 was better than others with maximum
51
52 276 correlation coefficient (R). So SG-D1 method was applied to the spectrum
53
54 277 preprocessing in the study. The profile of the raw NIRS and corresponding SG-D1 of
55
56 278 a fish is shown in Fig.2. It could be found that the raw spectra were smoothed and
57
58 279 weak peaks were enhanced after the application of SG-D1 preprocessing methods.

59 280 **3.3. Different PLS models**

60

1
2
3
4 281 The full spectrum range from 4000 to 10000 cm^{-1} was used. PLS model with the
5
6 282 full spectrum and iPLS model were obtained in sequence. The results are respectively
7
8 283 shown in the Fig.4 and Fig.5, where $R=0.8087$ and 0.8017 respectively in the
9
10 284 prediction sets. The performances of the two models were unsatisfactory, so Si-PLS
11
12 285 model was further used. Si-PLS was divided into 15, 16, 17,..., 21 intervals combined
13
14 286 with 5 to 9 subintervals as seen in Table 2. The optimal combination of intervals and
15
16 287 the number of PLS factor was optimized by cross validation. The best performance
17
18 288 was chosen according to the lowest root mean square error (RMSE). The best results
19
20 289 obtained by Si-PLS are shown in bold and italic characters from Table 2. Scatter plots
21
22 290 of Si-PLS model are shown in Fig.6. Seven spectra subintervals from the spectral
23
24 291 regions were selected by Si-PLS model as seen from Fig.7, including 5142.9-5428.6
25
26 292 cm^{-1} , 6571.3-7142.7 cm^{-1} , 7428.4-7999.8 cm^{-1} and 8856.9-9428.3 cm^{-1} . All the
27
28 293 ranges have 523 variables out of the 1557 variables. The selection was in accordance
29
30 294 with the group active spectral region in general. The spectra between (5142.9-5428.6
31
32 295 cm^{-1}) showed peak at 5169 cm^{-1} was associated with O–H stretching and combination,
33
34 296 which indicates the absorption peak of the water, at 5421 cm^{-1} associated with C–H
35
36 297 first overtone. The spectra (6571.3-7142.7 cm^{-1}) were obtained at 6861 cm^{-1} and 6852
37
38 298 cm^{-1} both associated with C-H stretching, at 7030 cm^{-1} associated with O–H first
39
40 299 overtone(Hunter, Kourtellis et al. 2011, Teye, Huang et al. 2014) , at 8000~8800 cm^{-1}
41
42 300 associated with C–H second overtone(Atta 2013). These spectral regions are typical
43
44 301 for fat, fatty acid and water in the fish(Atta 2013, Teye, Huang et al. 2014), which
45
46 302 have a close relationship with the freshness.

303 **3.4. SVMR models**

47
48 304 SVMR model with synergy intervals partial least squares (to form Si-SVMR
49
50 305 model) and SVMR model with the full spectra were also applied in this work. The top
51
52 306 priority was the choice of kernel function for modeling SVMR. Because mapping the
53
54 307 original data X nonlinearly into a higher dimensional feature space is implemented by
55
56 308 a kernel function(Chauchard, Cogdill et al. 2004). RBF kernel was used in the study
57
58 309 referring to the previous work (Gunasekaran, Paulsen et al. 1985). In order to get a
59
60 310 better performance, the penalty parameter C and kernel parameter γ have to be

1
2
3
4 311 optimized. The optimal performance of SVMR models was superior with penalty
5 312 parameter $C = 9.2674$ and kernel parameter $\gamma = 0.01$ (setting by γ in kernel function
6 313 RBF) in the work. PCA was used for data dimension reduction. Then 3 PCs of both
7 314 the full spectra and the joint intervals were as the input of the models. The result of
8 315 SVMR model with the full spectra is shown in Fig.8. SVMR model had a correlation
9 316 coefficient of 0.9410 in the calibration set and 0.9192 in prediction set, with
10 317 RMSECV=0.03177 and RMSEP= 0.03656 respectively, which displayed a good
11 318 performance but under fitted in the prediction model. Besides, the result of Si-SVMR
12 319 model was shown in Fig.9. From Fig.9, $R = 0.9595$ for the calibration set and 0.9374
13 320 for the prediction set, with RMSECV = 0.02710 and RMSEP = 0.03653 respectively,
14 321 which indicated an excellent performance of the prediction model. The predictive
15 322 values of Si-SVMR model and the measured K values from the prediction set are
16 323 shown in Table 3. The average relative error is 0.084. The model has a relatively large
17 324 error for the prediction of K value. But for the freshness discrimination the error is
18 325 still relatively reasonable. The first fresh sample was predicted as the secondary
19 326 freshness with $K = 0.2335$. The 30th secondary fresh sample was estimated as the
20 327 inedible object with $K = 0.4232$. And 5 inedible samples were predicted as the
21 328 secondary freshness ($20\% < K < 40\%$). Then Si-SVMR model has an accuracy of 87%
22 329 for the freshness discrimination. The prediction accuracy of K value near the critical
23 330 value has a great influence for the freshness discrimination. The prediction accuracy
24 331 of model still needs to be optimized.

25
26
27
28
29
30
31
32
33
34
35
36
37
38
39
40
41
42
43 332 As shown in Table 4. Si-SVMR was compared with different PLS models and
44 333 SVMR model with the full spectra. It was obvious that i-PLS model had the worst
45 334 generalization performance among the six. It is possible that some important
46 335 information were left out with the single interval. In the contrast, PLS model with the
47 336 full spectra which included all the spectra had more noise and redundant information,
48 337 which deprived the performance of the model. Si-PLS model merged together the
49 338 advantages of i-PLS and PLS, where as much as useful information remained and
50 339 noises were eliminated. So Si-PLS model was better than i-PLS and PLS models.
51 340 Even so, the performance of PLS models are inferior to SVMR models. One of
52
53
54
55
56
57
58
59
60

1
2
3 341 reasons is that two SVMR models belong to the non-linear recognition model while
4
5 342 Si-PLS model used here belong to the linear recognition model (Godoy, Vega et al.
6
7 343 2014). Generally, nonlinear models have significantly stronger self-learning ability in
8
9 344 the training process than the linear model. In fact there are also some potential
10
11 345 nonlinear relationship between spectral data and chemical measurements. So the
12
13 346 performance of the two SVMR models was better than the three PLS models.
14
15 347 Si-SVMR model had the best generalization performance of the six. It is possible that
16
17 348 the full spectra region contains more noise and redundant information, which weaken
18
19 349 the predictive performance of the model. Conversely Si-SVMR selected multiple
20
21 350 spectral sub-intervals that are informative and irrelevant information eliminated that
22
23 351 could deprive the performance of the model. Besides, the Si-SVMR model with the
24
25 352 less wave numbers is more efficient than SVMR model. When all the above factors
26
27 353 are taken into account, NIRS combined with Si-SVMR model was more suitable for
28
29 354 the detection of K value of fish.

30 355 **4.0 Conclusions**

31
32 356 This study shows that FT-NIRS coupled with chemometrics techniques could be
33
34 357 used for the quantitative prediction of K value of silver chub during the cold storage.
35
36 358 The eye of the silver chub is a feasible location for the detection by NIR spectroscopy,
37
38 359 due to the simple structure of fish eyes, the constant location and close relationship
39
40 360 with the fish freshness during the cold storage. The chemometrics treatment by
41
42 361 (Si-PLS, SVMR and Si-SVMR) of spectral data was faster, simpler and more
43
44 362 convenient than HPLC. Si-SVMR model had the best performance with a correlation
45
46 363 coefficient of 95.59% in the calibration set and 93.74% in prediction set, which
47
48 364 showed that NIRS together with Si-SVMR model has a high potential for the
49
50 365 prediction of K value in silver chubs during the cold storage. Although the
51
52 366 performance of Si-SVMR model needs to be further improved, the study could
53
54 367 provide a reference for the quantitative analysis of the fish freshness by near infrared
55
56 368 spectroscopy.

56 369 **Acknowledgements**

57
58 370 The authors wish to acknowledge the financial assistance provided by the
59
60

1
2
3 371 National Natural Science Foundation of China (No.31071549), Special Fund for
4 372 Agro-scientific Research in the Public Interest (No.201003008), Priority Academic
5 373 Program Development of Jiangsu Higher Education Institutes (PAPD).
6
7
8

9 374 **References**

10 375 Alimelli, A., G. Pennazza, M. Santonico, R. Paolesse, D. Filippini, A. D'Amico, I.
11 376 Lundström and C. Di Natale (2007). "Fish freshness detection by a computer screen
12 377 photoassisted based gas sensor array." Analytica chimica acta **582**(2): 320-328.

13 378 Alves, J. C. L. and R. J. Poppi (2013). "Biodiesel content determination in diesel fuel
14 379 blends using near infrared (NIR) spectroscopy and support vector machines (SVM)."
15 380 Talanta **104**: 155-161.

16 381 Atta, K. (2013). "Morphological, anatomical and histological studies on the olfactory
17 382 organs and eyes of teleost fish: *Anguilla anguilla* in relation to its feeding
18 383 habits." The Journal of Basic & Applied Zoology **66**(3): 101-108.

19 384 Bøknæs, N., K. N. Jensen, C. M. Andersen and H. Martens (2002). "Freshness
20 385 assessment of thawed and chilled cod fillets packed in modified atmosphere using
21 386 near-infrared spectroscopy." LWT-Food Science and Technology **35**(7): 628-634.

22 387 Bizri, M., J.-F. Bouhours, D. Garin and R. Got (1985). "Effect of acclimation
23 388 temperature on K_m values towards GDP-mannose of the
24 389 microsomal dolichol phosphate mannosyltransferase activity of trout liver (*Salmo*
25 390 *gairdnerii*)." Comparative Biochemistry and Physiology Part B:
26 391 Comparative Biochemistry **80**(4): 693-696.

27 392 Buerck, J., S. Roth, K. Kraemer, M. Scholz and N. Klaas (2001). "Application of a
28 393 fiber-optic NIR-EFA sensor system for in situ monitoring of aromatic hydrocarbons in
29 394 contaminated groundwater." Journal of hazardous materials **83**(1): 11-28.

30 395 Chauchard, F., R. Cogdill, S. Roussel, J. Roger and V. Bellon-Maurel (2004).
31 396 "Application of LS-SVM to non-linear phenomena in NIR spectroscopy: development
32 397 of a robust and portable sensor for acidity prediction in grapes." Chemometrics and
33 398 Intelligent Laboratory Systems **71**(2): 141-150.

34 399 Chen, Q., J. Ding, J. Cai and J. Zhao (2012). "Rapid measurement of total acid
35 400 content (TAC) in vinegar using near infrared spectroscopy based on efficient variables
36
37
38
39
40
41
42
43
44
45
46
47
48
49
50
51
52
53
54
55
56
57
58
59
60

- 1
2
3 401 selection algorithm and nonlinear regression tools." Food chemistry **135**(2): 590-595.
- 4
5 402 Chen, Q., J. Zhao, S. Chaitep and Z. Guo (2009). "Simultaneous analysis of main
6
7 403 catechins contents in green tea (< i> Camellia sinensis</i>(L.)) by Fourier transform
8
9 404 near infrared reflectance (FT-NIR) spectroscopy." Food Chemistry **113**(4): 1272-1277.
- 10
11 405 Chen, Q., J. Zhao, C. Fang and D. Wang (2007). "Feasibility study on identification of
12
13 406 green, black and Oolong teas using near-infrared reflectance spectroscopy based on
14
15 407 support vector machine (SVM)." Spectrochimica Acta Part A: Molecular and
16
17 408 Biomolecular Spectroscopy **66**(3): 568-574.
- 18
19 409 Devos, O., C. Ruckebusch, A. Durand, L. Duponchel and J.-P. Huvenne (2009).
20
21 410 "Support vector machines (SVM) in near infrared (NIR) spectroscopy: Focus on
22
23 411 parameters optimization and model interpretation." Chemometrics and Intelligent
24
25 412 Laboratory Systems **96**(1): 27-33.
- 26
27 413 Dowlati, M., M. de la Guardia, M. Dowlati and S. S. Mohtasebi (2012). "Application
28
29 414 of machine-vision techniques to fish-quality assessment." TrAC Trends in Analytical
30
31 415 Chemistry **40**: 168-179.
- 32
33 416 Dowlati, M., S. S. Mohtasebi, M. Omid, S. H. Razavi, M. Jamzad and M. de la
34
35 417 Guardia (2013). "Freshness assessment of gilthead sea bream (< i> Sparus aurata</i>)
36
37 418 by machine vision based on gill and eye color changes." Journal of Food Engineering
38
39 419 **119**(2): 277-287.
- 40
41 420 FuBin, X., H. XingYi, D. Ran, G. HaiYang, Y. LiYa and D. Huang (2012). "Freshness
42
43 421 evaluation model of Pseudosciaena crocea based on near-infrared spectra." Journal of
44
45 422 Food Safety and Quality **3**(6): 644-648.
- 46
47 423 Gil, L., J. M. Barat, E. Garcia-Breijo, J. Ibañez, R. Martínez-Máñez, J. Soto, E. Llobet,
48
49 424 J. Brezmes, M. Aristoy and F. Toldrá (2008). "Fish freshness analysis using metallic
50
51 425 potentiometric electrodes." Sensors and Actuators B: Chemical **131**(2): 362-370.
- 52
53 426 Godoy, J. L., J. R. Vega and J. L. Marchetti (2014). "Relationships between PCA and
54
55 427 PLS-regression." Chemometrics and Intelligent Laboratory Systems **130**: 182-191.
- 56
57 428 Gunasekaran, S., M. Paulsen and G. Shove (1985). "Optical methods for
58
59 429 nondestructive quality evaluation of agricultural and biological materials." Journal of
60
61 430 Agricultural Engineering Research **32**(3): 209-241.

- 1
2
3 431 Huang, X., J. Xin and J. Zhao (2011). "A novel technique for rapid evaluation of fish
4 freshness using colorimetric sensor array." Journal of Food Engineering **105**(4):
5 632-637.
6
7
8
9 434 Hunter, M. T., A. G. Kourtellis, C. D. Ziomek and W. B. Mikhael (2011).
10 "Fundamentals of modern spectral analysis." Instrumentation & Measurement
11 Magazine, IEEE **14**(4): 12-16.
12
13 436
14 437 Jamshidi, B., S. Minaei, E. Mohajerani and H. Ghassemian (2012). "Reflectance
15 Vis/NIR spectroscopy for nondestructive taste characterization of Valencia oranges."
16 Computers and Electronics in Agriculture **85**: 64-69.
17
18
19 439
20 440 Kamalakanth, C., J. Ginson, J. Bindu, R. Venkateswarlu, S. Das, O. Chauhan and T.
21 Gopal (2011). "Effect of high pressure on K-value, microbial and sensory
22 characteristics of yellowfin tuna (*Thunnus albacares*) chunks in EVOH films
23 during chill storage." Innovative Food Science & Emerging Technologies **12**(4):
24 451-455.
25
26
27 443
28 444
29 445 Khodabux, K., M. S. S. L'Omelette, S. Jhaumeer-Laulloo, P. Ramasami and P.
30 Rondeau (2007). "Chemical and near-infrared determination of moisture, fat and
31 protein in tuna fishes." Food chemistry **102**(3): 669-675.
32
33 447
34 448 Kimiya, T., A. H. Sivertsen and K. Heia (2013). "VIS/NIR spectroscopy for
35 non-destructive freshness assessment of Atlantic salmon (*Salmo salar* L.)
36 fillets." Journal of Food Engineering **116**(3): 758-764.
37
38
39 450
40 451 Li, J., L. Wang, X. Zhang and H. Li (2013). "Rapid Assessment of the Freshness of
41 Large Yellow Croaker by Near Infrared Spectroscopy Combined with PLS Methods."
42 Journal of Chinese Institute of Food Science and Technology **13**(6): 209-215.
43
44 453
45 454 Losada, V., C. Piñeiro, J. Barros-Velázquez and S. P. Aubourg (2005). "Inhibition of
46 chemical changes related to freshness loss during storage of horse mackerel (*Trachurus trachurus*)
47 in slurry ice." Food Chemistry **93**(4): 619-625.
48
49 456
50 457 Lougovois, V. P., E. R. Kyranas and V. R. Kyrana (2003). "Comparison of selected
51 methods of assessing freshness quality and remaining storage life of iced gilthead sea
52 bream (*Sparus aurata*)."
53 Food Research International **36**(6): 551-560.
54
55 459
56 460 Nicolai, B. M., K. Beullens, E. Bobelyn, A. Peirs, W. Saeys, K. I. Theron and J.

- 1
2
3
4 461 Lammertyn (2007). "Nondestructive measurement of fruit and vegetable quality by
5 462 means of NIR spectroscopy: A review." Postharvest Biology and Technology **46**(2):
6 463 99-118.
- 7
8
9 464 Nollet, L. and F. Toldra (2010). *Seafood and seafood product analysis*, CRC Press,
10 465 Boca Raton, FL, USA.
- 11
12 466 Pons-Sánchez-Cascado, S., M. Vidal-Carou, M. Nunes and M. Veciana-Nogues
13 467 (2006). "Sensory analysis to assess the freshness of Mediterranean anchovies (< i>
14 468 *Engraulis encrasicolus*</i>) stored in ice." Food Control **17**(7): 564-569.
- 15
16
17
18 469 Porfire, A., L. Rus, A. L. Vonica and I. Tomuta (2012). "High-throughput
19 470 NIR-chemometric methods for determination of drug content and pharmaceutical
20 471 properties of indapamide powder blends for tableting." Journal of pharmaceutical and
21 472 biomedical analysis **70**: 301-309.
- 22
23
24
25
26 473 Ribeiro, T., S. Raja, A. S. Rodrigues, F. Fernandes, C. Baleizão and J. P. S. Farinha
27 474 (2014). "NIR and visible perylenediimide-silica nanoparticles for laser scanning
28 475 bioimaging." Dyes and Pigments.
- 29
30
31 476 Ruiz-Rico, M., A. Fuentes, R. Masot, M. Alcañiz, I. Fernández-Segovia and J. M.
32 477 Barat (2013). "Use of the voltammetric tongue in fresh cod (< i> *Gadus morhua*</i>)
33 478 quality assessment." Innovative Food Science & Emerging Technologies **18**: 256-263.
- 34
35
36
37 479 Teye, E., X.-y. Huang, W. Lei and H. Dai (2014). "Feasibility study on the use of
38 480 Fourier transform near-infrared spectroscopy together with chemometrics to
39 481 discriminate and quantify adulteration in cocoa beans." Food Research International
40 482 **55**: 288-293.
- 41
42
43
44 483 Teye, E., X. Huang, H. Dai and Q. Chen (2013). "Rapid differentiation of Ghana
45 484 cocoa beans by FT-NIR spectroscopy coupled with multivariate classification."
46 485 Spectrochimica Acta Part A: Molecular and Biomolecular Spectroscopy **114**: 183-189.
- 47
48
49 486 Tito, N., T. Rodemann and S. Powell (2012). "Use of near infrared spectroscopy to
50 487 predict microbial numbers on Atlantic salmon." Food microbiology **32**(2): 431-436.
- 51
52
53
54 488 Watanabe, E., Y. Tamada and N. Hamada-Sato (2005). "Development of quality
55 489 evaluation sensor for fish freshness control based on< i> K</i>< sub> I</sub> value."
56 490 Biosensors and Bioelectronics **21**(3): 534-538.
- 57
58
59
60

- 1
2
3
4 491 Wei, Z. J. L. X. W. and X. Wu (2007). "Measurment of Bio-impedance Characteristic
5 492 of Freshwater Fish Based on Virtual Instrument [J]." Transactions of the Chinese
6
7 493 Society for Agricultural Machinery **9**: 028.
8
9 494 Xu, L., D. Xie and F. Fan (2011). "Effects of Pretreatment Methods and Bands
10 495 Selection on Soil Nutrient Hyperspectral Evaluation." Procedia Environmental
11 496 Sciences **10**: 2420-2425.
12
13 497 Zaragoza, P., S. Ribes, A. Fuentes, J.-L. Vivancos, I. Fernández-Segovia, J. V. Ros-Lis,
14 498 J. M. Barat and R. Martínez-Máñez (2012). "Fish freshness decay measurement with
15 499 a colorimetric array." Procedia Engineering **47**: 1362-1365.
16
17
18
19
20 500 Zhang, F., S. Xu and Z. Wang (2011). "Pre-treatment optimization and properties of
21 501 gelatin from freshwater fish scales." Food and Bioproducts Processing **89**(3):
22 502 185-193.
23
24
25
26
27

28 Tables

29
30 505 Table 1 The performance of Si-PLS model with different preprocessing methods

Methods	R _{cal}	R _{pre}	PCs
SG	0.8669	0.8675	8
SNV	0.8338	0.8117	8
D1	0.8753	0.8779	8
D2	0.8274	0.7731	8
MSC	0.8322	0.8156	8
Centralization	0.8669	0.8675	8
SG-D1	0.8880	0.8776	8

31
32
33
34
35
36
37
38
39
40
41
42
43
44 506

45
46 507 Table 2 Calibration results by Si-PLS model with different spectral range selection

Number of intervals	PCs	Selected intervals	RMSECV	RMSEP
15	8	1,4,9,10,12,13,5,7	0.0446	0.0504
16	8	4,8,9,10,13,14,1,7,11	0.0453	0.0512
17	8	4,8,9,11,14	0.0458	0.0489
18	8	4,5,8,9,7,15	0.0454	0.0481
19	8	5,10,9,13,12,17,16	0.0454	0.0499

20	8	5,9,13,11,16,17	0.0474	0.0464
21	8	5,10,11,14,15,16,17	0.0421	0.0443
22	8	5,6,1,12,10,13,14,18	0.0463	0.0515
23	8	6,11,12,14,19,23	0.0456	0.0503
24	8	6,11,13,16,20	0.0467	0.0496
25	8	6,12,13,16,21,1,5	0.0432	0.0553

508

509

Table 3 The error analysis of measured and predictive K values in Si-SVMR

510

prediction set				
Sample number	Measured K value	Predictive value	Absolute error	Relative error
1	0.1910	0.2335	0.0425	0.2223
2	0.2026	0.2089	0.0063	0.0312
3	0.2081	0.2150	0.0069	0.0331
4	0.2117	0.2699	0.0582	0.2750
5	0.2250	0.2010	0.0240	0.1067
6	0.2300	0.2151	0.0149	0.0648
7	0.2364	0.2843	0.0479	0.2028
8	0.2409	0.2609	0.0200	0.0830
9	0.2568	0.2686	0.0118	0.0461
10	0.2641	0.2723	0.0082	0.0312
11	0.2690	0.3255	0.0565	0.2101
12	0.2739	0.3316	0.0578	0.2109
13	0.2799	0.3335	0.0536	0.1915
14	0.2861	0.2968	0.0107	0.0375
15	0.2906	0.3053	0.0147	0.0505
16	0.2946	0.2975	0.0029	0.0099
17	0.2993	0.3470	0.0477	0.1593
18	0.3025	0.3148	0.0123	0.0408
19	0.3135	0.3547	0.0412	0.1313

1
2
3
4
5
6
7
8
9
10
11
12
13
14
15
16
17
18
19
20
21
22
23
24
25
26
27
28
29
30
31
32
33
34
35
36
37
38
39
40
41
42
43
44
45
46
47
48
49
50
51
52
53
54
55
56
57
58
59
60

1					
2					
3					
4	20	0.3204	0.3272	0.0068	0.0212
5					
6	21	0.3306	0.3341	0.0035	0.0107
7					
8	22	0.3349	0.3526	0.0177	0.0528
9					
10	23	0.3395	0.3504	0.0109	0.0321
11					
12	24	0.3434	0.3736	0.0302	0.0878
13					
14	25	0.3491	0.3714	0.0223	0.0640
15					
16	26	0.3526	0.3887	0.0360	0.1022
17					
18	27	0.3689	0.3958	0.0269	0.0730
19					
20	28	0.3712	0.2989	0.0723	0.1948
21					
22	29	0.3750	0.3701	0.0049	0.0131
23					
24	30	0.3791	0.4232	0.0441	0.1164
25					
26	31	0.3914	0.3610	0.0304	0.0777
27					
28	32	0.3971	0.3798	0.0173	0.0436
29					
30	33	0.4055	0.3663	0.0392	0.0966
31					
32	34	0.4075	0.3861	0.0214	0.0524
33					
34	35	0.4170	0.4133	0.0037	0.0088
35					
36	36	0.4214	0.3909	0.0305	0.0724
37					
38	37	0.4292	0.3925	0.0367	0.0855
39					
40	38	0.4333	0.3950	0.0382	0.0882
41					
42	39	0.4385	0.4342	0.0042	0.0097
43					
44	40	0.4405	0.4116	0.0289	0.0656
45					
46	41	0.4503	0.4095	0.0408	0.0905
47					
48	42	0.4539	0.4727	0.0188	0.0414
49					
50	43	0.4566	0.4077	0.0488	0.1070
51					
52	44	0.4586	0.4266	0.0320	0.0698
53					
54	45	0.4603	0.4242	0.0361	0.0784
55					
56	46	0.4634	0.4071	0.0563	0.1215
57					
58	47	0.4774	0.4409	0.0364	0.0763
59					
60	48	0.4809	0.4573	0.0237	0.0492

49	0.4850	0.4797	0.0053	0.0109
50	0.4892	0.4103	0.0789	0.1612
51	0.4923	0.4757	0.0166	0.0337
52	0.4972	0.4176	0.0796	0.1600
53	0.5100	0.5203	0.0103	0.0202
54	0.5189	0.4813	0.0376	0.0724
55	0.5201	0.5104	0.0097	0.0187
Average	0.3661	0.3635	0.0290	0.0840
value				

511

512

513

514

515 Table 4 Results of training and predicting based on SVMR and Bi-PLS model

Regression model	number of variable	Principal component factors	The training set		The prediction set	
			r	RMSECV	r	RMSEP
PLS	1557	8	0.8289	0.0512	0.8087	0.0553
iPLS	92	5	0.8096	0.0532	0.8017	0.0554
Si-PLS	523	8	0.8880	0.0421	0.8776	0.0443
SVMR	1557	3	0.94104	0.031770	0.91919	0.036561
Si-SVMR	523	3	0.95947	0.027095	0.93743	0.036525

516

517

518

519

520

521

522

523

524

525

526

Figures

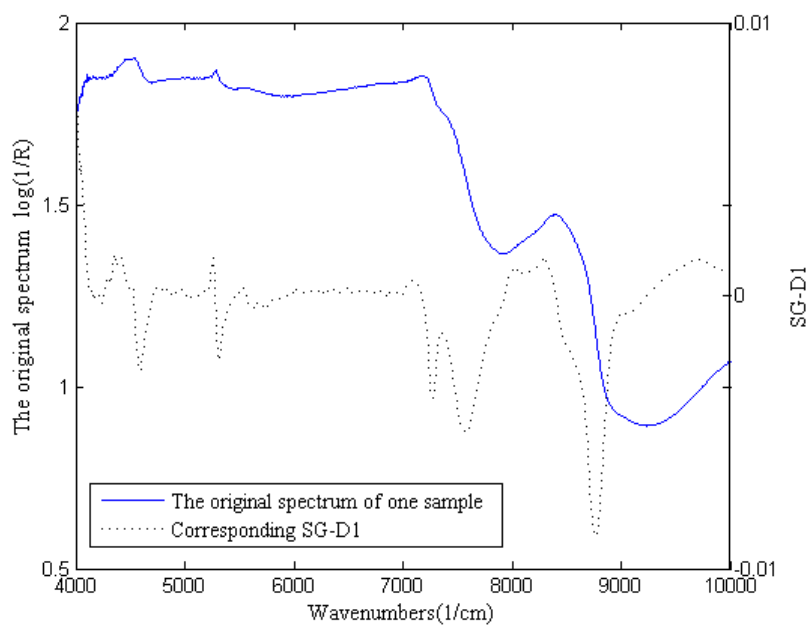


Fig 1. The raw NIR spectra and corresponding SG-D1 profile of a silver carp

527

528

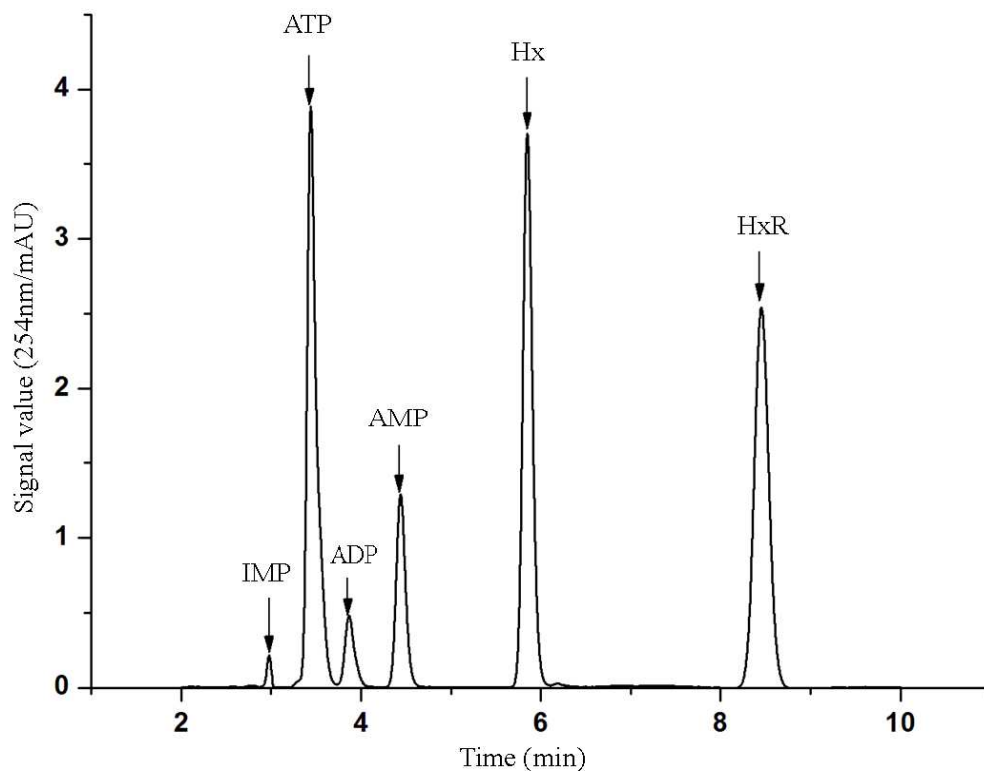


Fig 2. High Performance Liquid Chromatogram (HPLC) of the standard ATP-related compounds

529

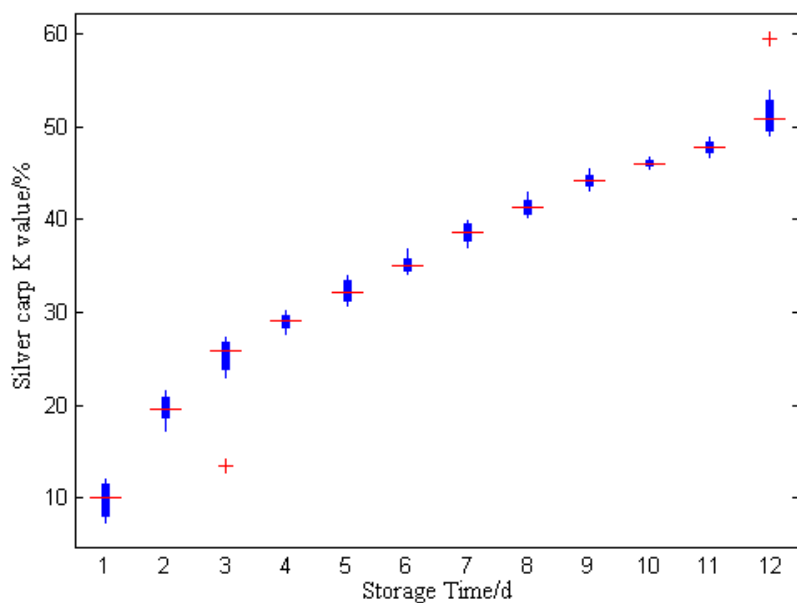


Fig. 3. The tendency of silver carp K values during the cold storage

530

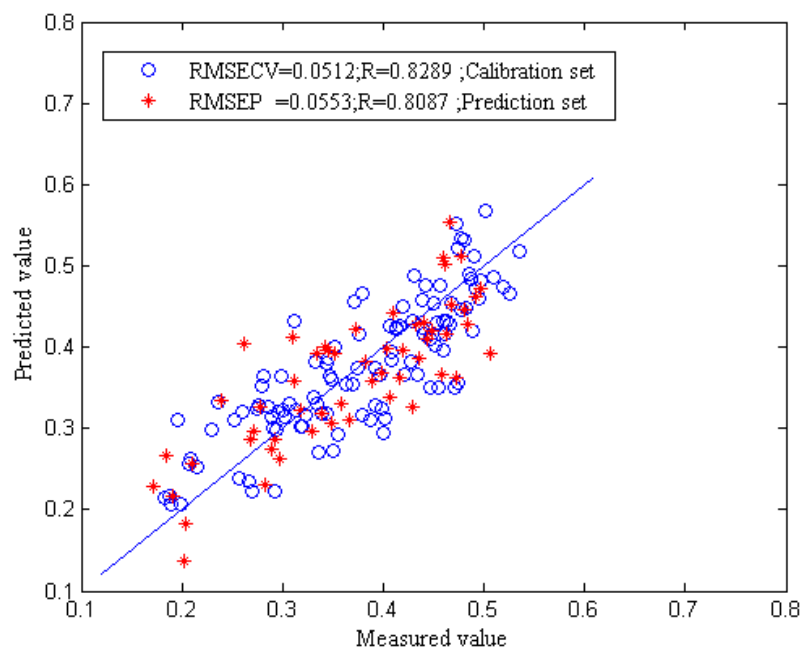


Fig. 4. Scatter plots of PLS model with NIR estimation and experimental K value

531

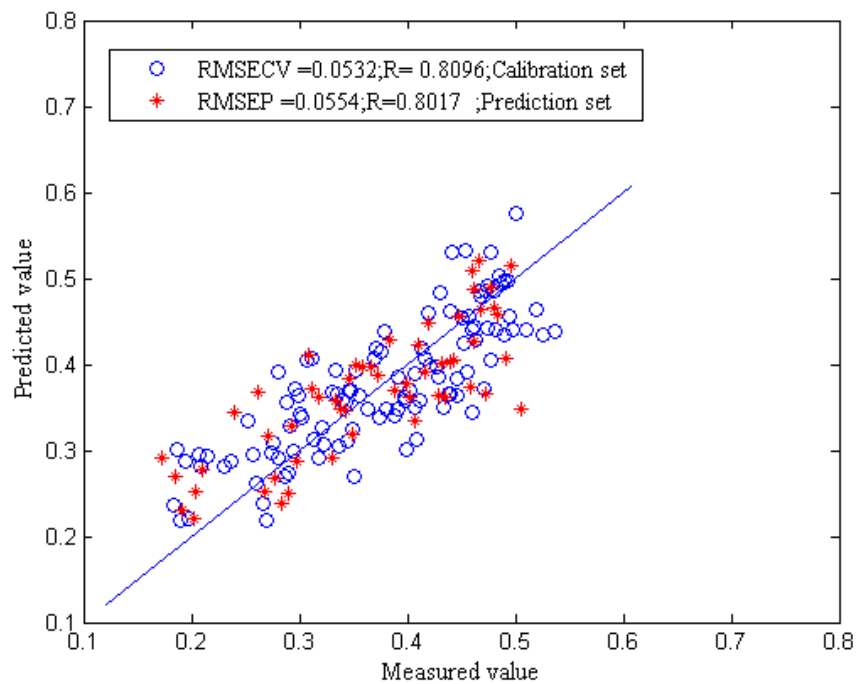


Fig.5. Scatter plots of i-PLS model with NIR estimation and experimental K value

532

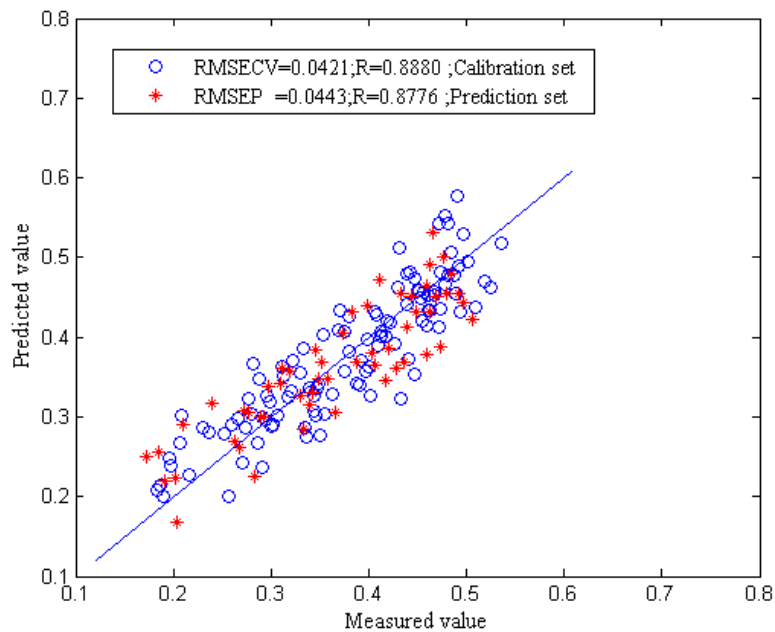
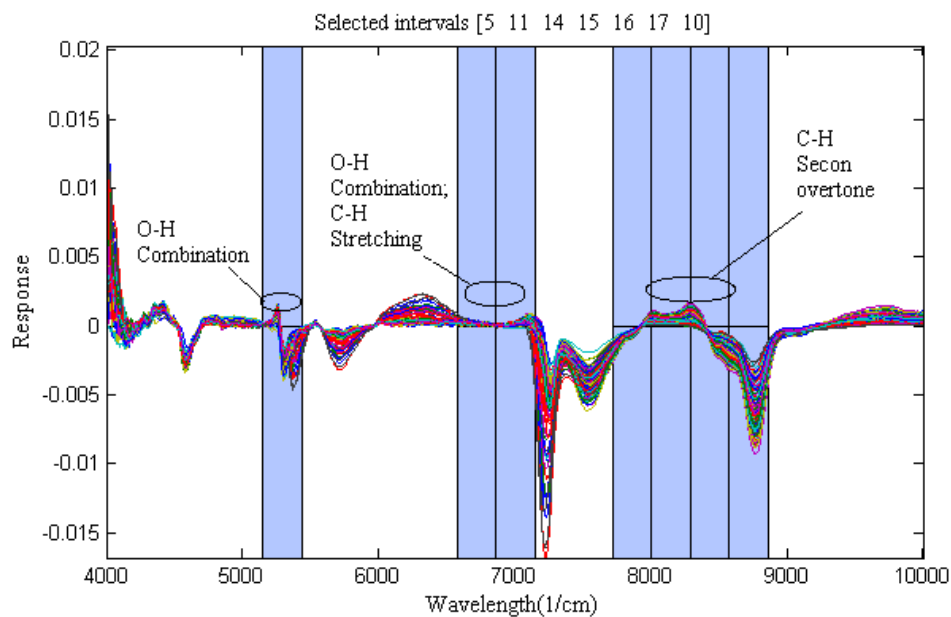


Fig.6. Scatter plots of Si-PLS model with NIR estimation and experimental K value

533



534

Fig 7. Si-PLS spectral selection at 8 PLS components

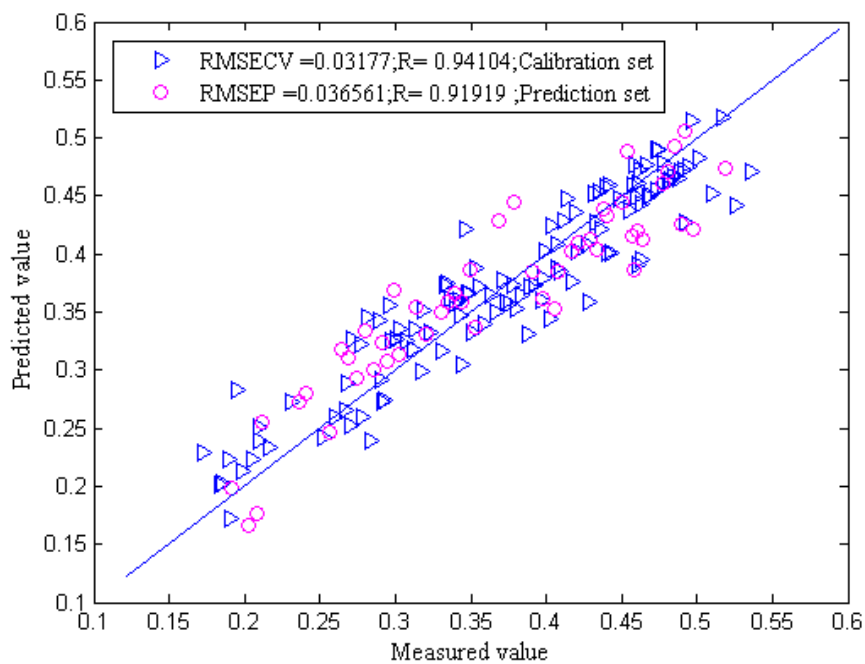


Fig 8. Scatter plots of SVMR model with NIR estimation and experimental K value

535

50
51
52
53
54
55
56
57
58
59
60

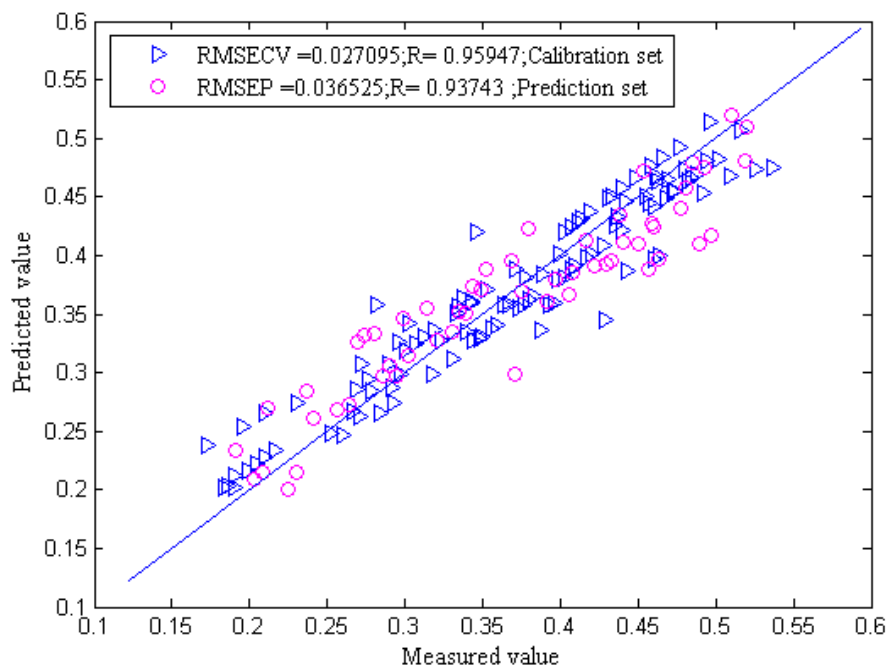
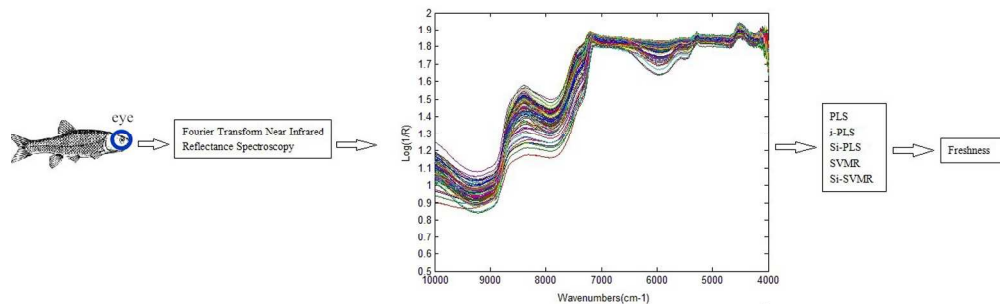


Fig 9. Scatter plots of Si-SVMR model with NIR estimation and experimental K value

536

537

538



344x138mm (300 x 300 DPI)

1
2
3
4
5
6
7
8
9
10
11
12
13
14
15
16
17
18
19
20
21
22
23
24
25
26
27
28
29
30
31
32
33
34
35
36
37
38
39
40
41
42
43
44
45
46
47
48
49
50
51
52
53
54
55
56
57
58
59
60